RSC Advances

ROYAL SOCIETY OF CHEMISTRY

www.rsc.org/advances

Graphical abstract

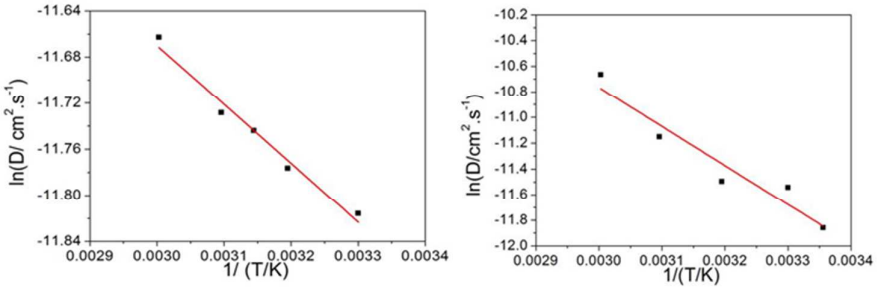

Two diffusion equations for both VO^{2+} and VO_2^+ ions in practical electrolyte (1.2 M V + 3.0 M H_2SO_4) have been established, which can be expressed by $D_{VO}^{2+} = 4\times10^{-5}$ exp (- 4240/RT) and D_{VO2}^{+}=0.18861exp (-25200/RT) (cm^2 s^{-1}).

Cite this: DOI: 10.1039/c0xx00000x

www.rsc.org/xxxxxx

ARTICLE TYPE

Temperature-related reaction kinetics of the vanadium (IV)/(V) redox couple in acidic solutions

Wenjun Wang, Xinzhuang Fan*, Jianguo Liu, Chuanwei Yan, Chaoliu Zeng*

Received (in XXX, XXX) Xth XXXXXXXXX 20XX, Accepted Xth XXXXXXXXX 20XX

DOI: 10.1039/b000000x

The temperature-related reaction kinetics of the VO_2^+/VO^{2+} redox couple on a graphite electrode in sulfuric acid solutions has been investigated by cyclic voltammetry and chronopotentiometry for a better understanding of the positive half-cell in a practical vanadium redox flow battery (VRFB). The elevated temperature facilitates the VO_2^+/VO^{2+} redox reaction, but without significant effect on its reversibility, and the reaction rate constants are calculated to be the order of magnitude of 10^{-3} cm s^{-1}. Additionally, the diffusion coefficient of both VO^{2+} and VO_2^+ ions tends to increase with increasing temperature with a diffusion activation energy of 4.24 kJ mol^{-1} for VO^{2+} and 25.2 kJ mol^{-1} for VO_2^+. On this basis, two diffusion equations for both VO^{2+} and VO_2^+ ions in sulfuric acid solutions have been established.

1. Introduction

In recent years, some renewable energy sources such as wind, solar and tidal power have been fast developed. However, the utilization of such unstable energy is still a problem. Thus, some new large-scale energy storage technologies such as redox-flow batteries, lithium-ion secondary batteries, lead-acid batteries, have been attempted to solve this problem.[1-3] As an interesting electrochemical conversion system, all vanadium redox flow battery (VRFB) applies four different oxidation states of vanadium ions to form two redox couples represented as VO_2^+/VO^{2+} and V^{2+}/V^{3+} which are separated as the anolyte and the catholyte with a piece of ion exchange membrane, and has been considered as a promising candidate for large-scale energy storage and power output due to the advantages like fast charging-discharging and long cycle life.[4-5] VRFB stores or releases electric energy through chemical changes of vanadium ions in concentrated sulfuric acid solutions, involving the oxidation or reduction processes and diffusion procedures of vanadium ions in electrolytes. Therefore, it is of great significance to understand thoroughly the reaction kinetics of VRFB for improving its electrochemical performances.

As important kinetic parameters, the reversibility and reaction rate of vanadium redox reactions have a significant effect on the electrochemical performances of VRFB.[6] Moreover, the diffusion of vanadium ions plays an important role in the electrode process due to the viscous electrolyte.[4] Additionally, the kinetic behavior of vanadium redox reactions is also strongly influenced by the variety of electrode surface state, [6-12] electrolyte concentration, [13-18] and temperature.[15,19] So far, extensive investigations have been given to the effects of electrode surface state and electrolyte concentration on the kinetic behavior of vanadium ions, especially the positive VO_2^+/VO^{2+} couple.[6-19] However, little attention has been paid to the effect of temperature on the kinetic behavior, in despite of its importance, and the scanty corresponding conclusion are also in controversy to a certain extent. For example, Liu *et al* have reported that higher temperature facilitates the oxidation reaction of VO^{2+}, [19] while Iwasa *et al* presented that increasing temperature contributes to a decrease in the reversibility of the VO_2^+/VO^{2+} couple on glassy carbon electrodes.[15] Although the diffusion coefficients of VO^{2+} and VO_2^+ ions have been measured mainly in very dilute electrolytes, [13, 20-22] their values are different, and also the effect of temperature on them is still unclear. Therefore, it is essential to examine extensively the effect of temperature on the reversibility and reaction rate of the VO_2^+/VO^{2+} couple and on the diffusion behavior of vanadium ions in sulfuric acid solutions.

In addition, the redox reaction mechanism of the VO_2^+/VO^{2+} couple is also an important topic in the investigation of the reaction kinetics of VRFB, but with limited reports available [23-26]. Recently, a series of investigations have been conducted in the present research group to understand thoroughly the reaction kinetics of the VO_2^+/VO^{2+} in acidic solutions. In a study of the oxidation reaction of VO^{2+} on a rotating graphite disk electrode by potentiodynamic polarization in sulfuric acid solutions, the present authors proposed a novel reaction mechanism to describe the oxidation of VO^{2+}, and further established a reaction kinetic equation.[27-28]

In this work, the effect of temperature on the reaction kinetics of the VO_2^+/VO^{2+} redox couple on a graphite electrode in sulfuric acid solutions has been investigated by cyclic voltammetry and chronopotentiometry for achieving a better understanding of the reactions occurring in the positive half-cell of a practical VRFB.

2. Experimental

2.1. Electrode preparation

A spectroscopically pure graphite rod (Sinosteel Shanghai Advanced Graphite Material Co. Ltd, China) with a working area

of around 0.28cm^2 was ground with down to 2000 grit silicon carbide papers, followed by polishing with a flanelle and thoroughly rinsing with alcohol before use.

2.2. Preparation of electrolyte solutions

All chemicals used in the experiments were analytically pure agents and all solutions were prepared with de-ionized water. 1.2 M $VOSO_4$ + 3.0 M H_2SO_4 solutions were made by dissolving $VOSO_4 \cdot nH_2O$ (n=2.82, according to the chemical precipitation method) in 3.0 M H_2SO_4. 1.2 M V (V) + 3.0 M H_2SO_4 solutions were obtained at the positive side of a single VRFB cell by charging. The VRFB cell had the same volume of V (IV) solution at the positive half-cell as at the negative half-cell, using a Nafion212 membrane (DuPont, USA) as the separator and a carbon felt (geometric area = 28cm^2) as the electrode material. The initial electrolytes at both half-cells were 1.2 M $VOSO_4$ + 3.0 M H_2SO_4 and the upper limit of the charge voltage was set at 1.65 V. The charge current was subsequently set as 1600, 1000, 600 and 300mA for a complete charge test.

2.3. Electrochemical measurements

A conventional three-electrode cell was used for electrochemical measurements with a spectroscopically pure graphite rod as the working electrode, a platinum plate as the counter electrode and a saturated calomel electrode (SCE) as the reference electrode. A salt bridge was used to decrease the liquid junction potential between the Luggin capillary and the working electrode. The Luggin capillary was as close as possible to the working electrode to reduce the solution resistance. Cyclic voltammograms (CV) and chronopotentiograms were obtained with a CHI730C Electrochemical Analysis Instrument (Shanghai Chenhua Instrument Co. Ltd, China) and a CorrTest Electrochemical Workstation (Wuhan CorrTest Instrument Co. Ltd, China), respectively. The operating temperature was controlled with a water bath. The CV measurements were carried out at temperatures from 10 to 50°C, while the chronopotentiograms were obtained at temperatures from 25 to 60°C due to that the temperature-controlling device can only support the experiments at above room temperature.

2.4. Viscosity characterization

The viscosity of the electrolytes was measured by a NDJ-5S digital torsion viscosimeter (Shanghai Ni Run Intelligent Technology Co. Ltd, China).

2.5. Analysis of cyclic voltammograms

The ratio of cathodic peak current (i_{pc}) to anodic peak current (i_{pa}) can be calculated from the cyclic voltammograms by the following equation: [29]

$$\frac{i_{pc}}{i_{pa}} = \frac{(i_{pc})_0}{i_{pa}} + \frac{0.485(i_{sp})_0}{i_{pa}} + 0.086 \quad (1)$$

where $(i_{pc})_0$ is the uncorrected cathodic peak current density with respect to the zero current baseline and $(i_{sp})_0$ is the current density at the switching potential.

For a totally irreversible process, the peak current density from the cyclic voltammograms can be presented as: [29]

$$i_p = 2.27\times10^{-4} nFC_b k_s exp\left[-\alpha n_a F\left(E_p - E^{O'}\right)/RT\right] \quad (2)$$

where i_p is the peak current density (A cm^{-2}), E_p is the peak potential (V), C_b is the bulk concentration of the electroactive species (mol L^{-1}), k_s is the standard heterogeneous rate constant (cm s^{-1}), α means the charge transfer coefficient, n_a is the number of electrons involved in the rate-limited step, $E^{O'}$ is the formal potential of the electrode, n is the electron transfer number of the electrode reaction and the other symbols such as F, R and T have their usual meanings.

For an irreversible electrode process, the peak current density is also given by: [29]

$$i_p = 4.958\times10^{-4} nFC_b D^{1/2} v^{1/2} \left(-\alpha n_a F/RT\right)^{1/2} \quad (3)$$

where v is the potential sweep rate (V s^{-1}), D the diffusion coefficient of the reactant (cm^2 s^{-1}).

Determined at various scan rates, a straight line of lni_p vs. (E_p-$E^{O'}$) by eqn. 2 can have an intercept proportional to k_s. Additionally, with a value of αn_a known, the value of the diffusion coefficient of ions can be calculated from the slope of the plot of i_p vs. $v^{1/2}$ by eqn. 3. Especially, $E^{O'}$ can be estimated from the cyclic voltammograms by [29]:

$$E^{O'} = \frac{\sum_{i=1}^{j}(E_{pa_i} + E_{pc_i})/2}{j} \quad (4)$$

where j is the total number of potential scan rates applied in the CV measurement, E_{pa} the anodic peak potential and E_{pc} the cathodic peak potential.

Additionally, in the present vanadium system, the ohmic resistance of the electrolyte has been measured to be around 0.14 Ω cm^2 by electrochemical impedance spectroscopy. Since the solution resistance is very small, it wasn't compensated in the CV measurements, and also not eliminated in the analyses and calculations based on the CV results.

3. Results and Discussion

3.1. Cyclic voltammograms and chronopotentiograms in V (IV) solutions

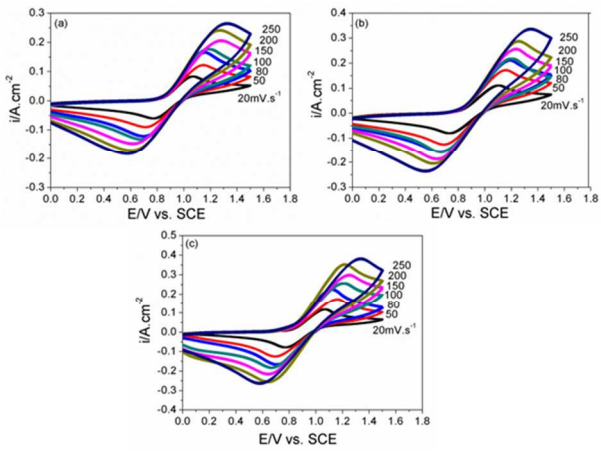

Fig. 1. Voltammograms on the graphite electrode in 1.2 M VOSO4+ 3.0 M H_2SO_4 solutions at 10°C (a), 30°C (b) and 50°C (c).

Table 1 Ratios of cathodic peak current (i_{pc}) to anodic peak current (i_{pa}) and the formal potential ($E^{O'}$) calculated from the cyclic voltammograms of Fig.1 for the VO_2^+/VO^{2+} redox reaction.

T/ °C	$E^{O'}$/V	i_{pc}/i_{pa}
10	0.940	1.16
20	0.940	1.17
30	0.935	1.17
40	0.945	1.15
50	0.935	1.14

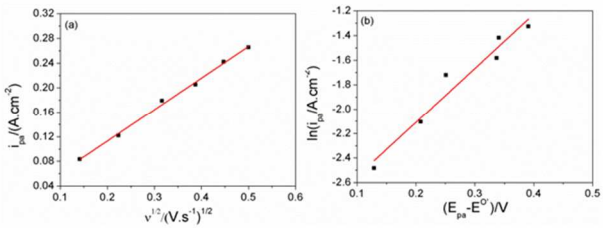

Fig. 2. Plots of i_{pa} vs. $v^{1/2}$ (a) and lni_{pa} vs. (E_{pa}-$E^{O'}$) (b) at 10°C for voltammograms in Fig. 1a.

Table 2 The rate constants of the oxidation reaction (k_s) and the diffusion coefficients of VO^{2+} ions ($D_{VO^{2+}}$) at different temperatures.

T/ °C	D/(10^{-6}cm^2.s^{-1})	k_s/(10^{-3}cm.s^{-1})
10	3.60	1.91
20	5.68	2.13
30	5.63	3.26
40	6.11	5.03
50	8.31	5.11

Fig. 1 illustrates the typical CV curves at different scan rates ranging from 20 to 250 mV s^{-1} in V (IV) solutions at various temperatures. All the separations between the oxidation and reduction peak potentials (ΔE_p) observed from Fig. 1 are much greater than 60mV, indicating that the VO_2^+/VO^{2+} redox reaction is irreversible.[29] The formal potential $E^{O'}$ at different temperatures can be calculated by eqn. 4, as listed in Table 1. The values of i_{pc} and i_{pa} can be also obtained from the CV curves in Fig. 1. According to eqn. 1, the mean values of i_{pc}/i_{pa} with various scan rates are calculated for all the temperatures (Table 1). Table 1 shows clearly that i_{pc}/i_{pa} change little with temperature, deducing that temperature has no significant effect on the reversibility of the VO_2^+/VO^{2+} redox reaction. It has been known that when the value of i_{pc}/i_{pa} is closer to 1 at the same scan rate, a more reversible reaction is expected.[29] In the present investigation, the values of i_{pc}/i_{pa} are slightly larger than 1, indicating an unfavorable reversibility of the VO_2^+/VO^{2+} redox reaction in V (IV) solutions, probably due to the fact that the graphite electrode used has a low activation. As shown in Fig. 2, the plot of i_{pa} vs. $v^{1/2}$ and the proportionality of lni_p vs. (E_p-$E^{O'}$) are obtained from the CV curves of Fig. 1a. The values of the anodic charge transfer coefficient (1-α) and the electron transfer number n_a have been estimated to be 0.53 and 1 in our previous work.[28] Through the two approximately linear curves, the values of k_s and $D_{VO^{2+}}$ are calculated according to eqs. (2) and (3), respectively, and are listed in Table 2. It can be seen that the values of the reaction rate constant k_s are of the order of magnitude of 10^{-3} cm.s^{-1} and increase with increasing temperature, indicating that a higher temperature facilitates the VO_2^+/VO^{2+} redox reaction. Furthermore, Except for the abnormal values at 20 and/or 30°C probably due to the differences in the electrode preparation procedures, $D_{VO^{2+}}$ goes up from 3.60×10^{-6} at 10°C to 8.31×10^{-6} cm^2 s^{-1} at 50°C, suggesting that the increase in temperature can promote the mobility of VO^{2+} ions in the sulfuric acid solutions.

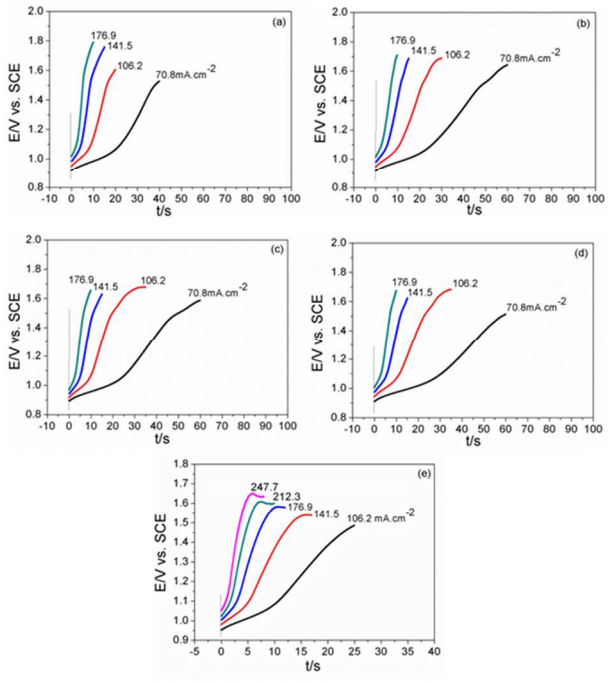

Fig. 3. Chronopotentiograms for the oxidation reaction of VO^{2+} on the graphite electrode under various temperatures. 30°C (a), 40°C (b), 45°C (c), 50°C (d) and 60°C (e).

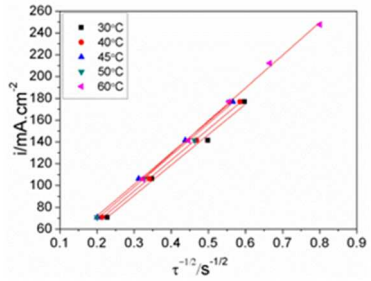

Fig. 4. The current density as a function of the reciprocal of the square root of the transition time for the oxidation reaction of VO^{2+}.

Table 3 The diffusion coefficients of VO^{2+} ions ($D_{VO^{2+}}$) calculated from Fig. 4 and the values of viscosity at different temperatures.

T/ °C	D/10^{-6}cm^2.s^{-1}	$\eta_{VO^{2+}}$ /mPa.s
30	7.39	3.18
40	7.68	2.56
45	7.94	2.4
50	8.06	2.24
60	8.61	-

CV is not an ideal quantitative method for the determination of some kinetic parameters based on peak heights. Thus, the diffusion coefficient of VO^{2+} ions is also measured with chronopotentiometry and calculated by Sand's equation.[30] Fig. 3 presents the chronopotentiograms for the oxidation reaction of

VO^{2+} at various temperatures in V (IV) solutions on the graphite electrode. For an irreversible or reversible reaction, Sand's equation can be given by:

$$\tau = \frac{n^2F^2\pi DC_b^{\ 2}}{4i^2} \quad (5)$$

where, τ, as the transition time, is the total time it takes before an abrupt change in the potential of the electrode, i the current density, and the other symbols such as n, F, D and C_b have their same meanings as the above. The values of τ are also determined as the transition time when the absolute values of the slope of the plots in Fig. 3 have an abrupt increase. The plots of i vs. $\tau^{-1/2}$ obtained from Fig. 3 are shown in Fig. 4 and the values of D_{VO}^{2+} can be calculated from the slopes of these plots, as listed in Table 3. D_{VO}^{2+} increases from 7.39×10^{-6} to 8.61×10^{-6} cm^2 s^{-1} at temperatures from 30 to 60°C. Moreover, as shown in Table 3, the viscosity (η) is reduced with increasing temperature, suggesting that the mobility of ions is facilitated with higher temperatures.

Table 4 The diffusion coefficient of VO^{2+} ions presented in some previous reports and the results from this work.

Electrode	T/ °C	Solution condition	$D_{VO}^{2+}/10^{-6}cm^2.s^{-1}$	Method	Reference
glassy carbon	25	$[VO^{2+}]$=0.03 M, $[H_2SO_4]$=4.2 M	1.0	Chronopotentiometry	[21]
graphite	25	$[VO^{2+}]$=0.5 M, $[H_2SO_4]$=3.0 M	1.86	Rotating-disc voltammetry	[22]
graphite	30	$[VO^{2+}]$=1.2 M, $[H_2SO_4]$=3.0 M	5.97	Cyclic voltammetry	This work
graphite	30	$[VO^{2+}]$=1.2 M, $[H_2SO_4]$=3.0 M	7.39	Chronopotentiometry	This work

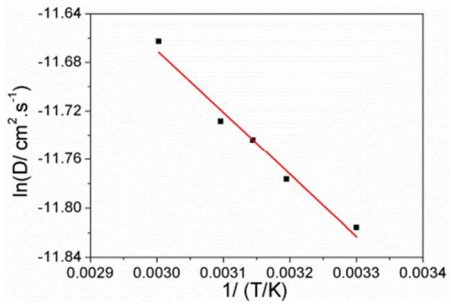

Fig. 5. The shift of ln$D(T)$ with $1/T$ for the anodic oxidation of VO^{2+} on the graphite electrode.

By a comparison of Tables 2 and 3 it can be seen that the values of D_{VO}^{2+} obtained from cyclic voltammetry and chronopotentiometry are of the same magnitude as 10^{-6} cm^2 s^{-1}, but with a smaller change with temperature observed for chronopotentiometry. A favorable result may come from chronopotentiometry owing to its good quantitative determination. Table 4 lists the values of D_{VO}^{2+} reported in some previous papers and the results from this work. It can be seen that the diffusion coefficients of VO^{2+} are all in the order of 10^{-6} cm^2 s^{-1}, but with larger values observed for the present investigation, probably due to the variety of carbon electrodes and electrolytes applied in the measurements. Moreover, it is noted that the values of the diffusion coefficient from the chronopotentiograms are generally higher than those from the CV curves, may attributed to the differences in both the experimental method and the calculation formula. Based on the chronopotentiometric results, the diffusion activation energy, E_D, can be obtained from the slope of the plot of ln$D(T)$ vs. $1/T$ by Arrhenius equation:[31]

$$D(T) = D_0 exp(-E_D / RT) \quad (6)$$

where D_0 is a temperature-independent factor (cm^2 s^{-1}), R and T have their usual meanings. The shift of ln$D$ *(T)* with *1/T* is shown as Fig. 5. Thus, the values of E_D and D_0 can be estimated as 4.24 kJ mol^{-1} and 4×10^{-5} cm^2 s^{-1}, respectively. Then, the diffusion coefficient of VO^{2+} can be expressed as follows:

$$D_{VO}^{2+} = 4\times10^{-5}\exp(-4240/RT) \quad (7)$$

3.2. Cyclic voltammograms and chronopotentiograms in V (V) solutions

Fig. 6 gives the typical CV curves at different scan rates ranging from 20 to 250 mV s^{-1} in V (V) solutions at various temperatures, As observed in V (IV) solutions, all the values of ΔE_p in V (V) solutions are significantly greater than 60 mV, suggesting that the VO_2^{+}/VO^{2+} redox reaction is irreversible. Table 5 presents the mean values of i_{pa}/i_{pc} and $E^{O'}$ calculated from the CV curves in Fig. 6. Since the smaller degree that the value of i_{pc}/i_{pa} (or i_{pa}/i_{pc}) deviates from 1 suggests a better reversibility for a redox reaction,[29] the values of i_{pa}/i_{pc} are much larger than 1, suggesting a worse reversibility of the VO_2^{+}/VO^{2+} redox reaction is obtained in V (V) solutions than in V (IV) solutions. Furthermore, the values of i_{pa}/i_{pc} for V(V) solutions decreasing with the increase of temperature suggests an improvement in the reversibility of the VO_2^{+}/VO^{2+} redox reaction in V (V) solution at higher temperature. However, it is noted that the values for V (IV) solution has few changes with the increase of temperature, may due to the better reversibility of the VO_2^{+}/VO^{2+} redox reaction in V (IV) solutions than that in V (V) solutions. Additionally, the values of k_s and D_{VO2}^{+} in V (V) solutions are calculated from the CV curves of Fig. 6 and listed in Table 6. Table 6 suggests that the value of D_{VO2}^{+} increases from 3.51×10^{-6} to 10.4×10^{-6} cm^2 s^{-1} and the value of k_s increases from 1.78×10^{-3} to 2.38×10^{-3}cm s^{-1} as temperature goes up. It can be concluded that a higher temperature quickens both the mobility of VO_2^{+} ions and the VO_2^{+}/VO^{2+} redox reaction.

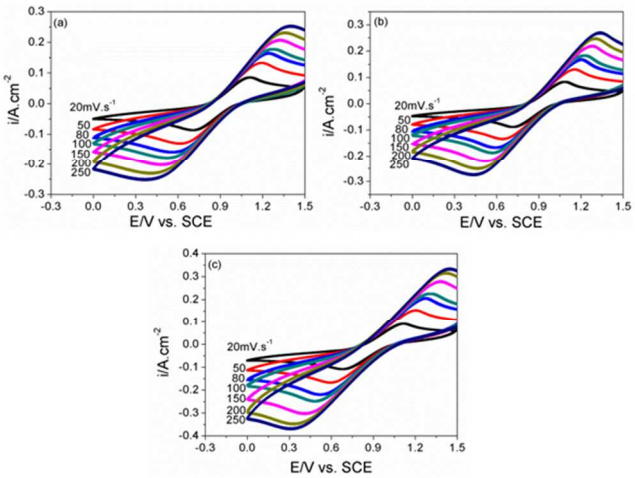

Fig. 6. Voltammograms on the graphite electrode in 1.2 M V (V)+ 3.0 M H_2SO_4 solutions at 10°C (a), 25°C (b) and 50°C (c).

Table 5 Ratios of anodic peak current (i_{pa}) to cathodic peak current (i_{pc}) and the formal potential ($E^{O'}$) calculated from the cyclic voltammograms of Fig. 6 for the VO_2^+/VO^{2+} redox reaction.

T/ °C	$E^{O'}$/V	i_{pa}/i_{pc}
10	0.899	1.46
25	0.898	1.38
50	0.892	1.35

Table 6 The rate constants of the vanadium redox reaction (k_s) and the diffusion coefficients of VO_2^+ ions (D_{VO2}^+) at different temperatures.

T/ °C	$D/10^{-6}$cm^2.s^{-1}	$k_s/10^{-3}$cm.s^{-1}
10	3.51	1.78
25	4.23	2.17
50	10.4	2.38

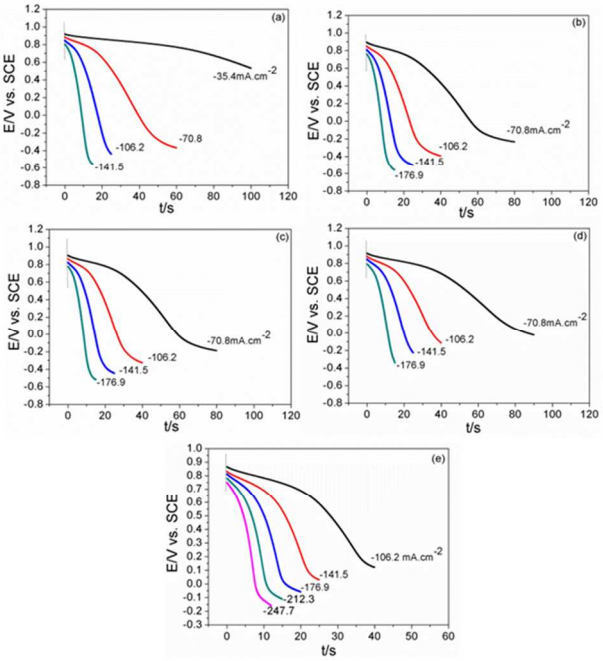

Fig. 7. Chronopotentiograms for the reduction reaction of VO_2^+ on the graphite electrode under various temperatures. 25°C (a), 30°C (b), 40°C (c), 50°C (d) and 60°C (e).

Furthermore, the diffusion coefficient of VO_2^+ ions is also measured with chronopotentiometry and calculated by Sand's equation.[30] Fig. 7 presents the chronopotentiograms for the reduction reaction of VO_2^+ at various temperatures in V (V) solutions on the graphite electrode and the corresponding plots of the current density (i) versus $\tau^{-1/2}$ are shown in Fig. 8. Table 7 lists the values of D_{VO2}^+ calculated from Sand's equation and the viscosity (η). D_{VO2}^+ increases from 7.07×10^{-6} to 23.4×10^{-6}cm^2 s^{-1} and the viscosity is decreased with increasing temperature, indicating that increasing temperature facilitates the mobility of ions in the V (V) solutions.

Table 8 lists the values of D_{VO2}^+ reported in references. It can be seen that the results obtained from cyclic voltammetry and chronopotentiometry are different to some extent, but with the same magnitude as 10^{-6} cm^2 s^{-1} at 25°C, which may be attributed to the discrepancy in the test conditions. However, chronopotentiometry is considered to be a more ideal method for the determination of the values of D_{VO2}^+ because of its better quantitative measurement.

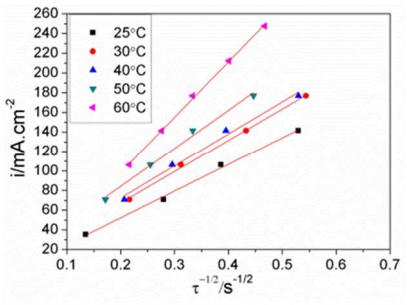

Fig. 8. The current density as a function of the reciprocal of the square root of the transition time for the cathodic reduction of VO_2^+.

Table 7 The diffusion coefficients of VO_2^+ ions (D_{VO2}^+) calculated from Fig. 8 and the values of viscosity at different temperatures.

T/ °C	$D/10^{-6}$cm^2.s^{-1}	η_{VO2}^+ /mPa.s
25	7.07	3.13
30	9.71	2.74
40	10.2	2.37
50	14.4	2.04
60	23.4	-

Table 8 The diffusion coefficient of VO_2^+ ions presented in some previous reports and the results from this work.

Electrode	T/°C	Solution condition	$D_{VO2}^+/10^{-6}$ cm^2.s^{-1}	Method	Reference
glassy carbon	25	$[VO_2^+]$=0.055M $[H_2SO_4]$=1.8 M	1.4	Cyclic voltammetry	[13]
gold electrode	25	$[VO_2^+]$=0.055 M, $[H_2SO_4]$=1.8 M	5.7	Cyclic voltammetry	[13]
Plastic formed carbon	25	$[VO_2^+]$=0.05 M, $[H_2SO_4]$=1.0 M	3.9	Cyclic voltammetry	[20]
glassy carbon	25	$[VO_2^+]$=0.05 M $[H_2SO_4]$=1.0 M	2.8	Cyclic voltammetry	[20]
pyrolytic graphite	25	$[VO_2^+]$=0.05 M, $[H_2SO_4]$=1.0 M	2.4	Cyclic voltammetry	[20]
glassy carbon	25	$[VO_2^+]$=0.03 M, $[H_2SO_4]$=5.0 M	1.0	Chronopotentiometry	[21]
graphite	25	$[VO_2^+]$=1.2 M, $[H_2SO_4]$=3.0 M	3.98	Cyclic voltammetry	This work
graphite	25	$[VO_2^+]$=1.2 M, $[H_2SO_4]$=3.0 M	7.07	Chronopotentiometry	This work

Based on Table 7, the change of ln$D$ (T) with 1/T for the V (V) reduction can be obtained, as shown in Fig. 9. According to eqn. 6, the values of E_D and D_0 for VO_2^+ ions can be estimated as 25.2 kJ mol^{-1} and 0.18861 cm^2 s^{-1}, respectively. Therefore, the diffusion coefficient of VO_2^+ can be expressed by the following equation:

D_{VO2+}= 0.18861exp (-25200/RT) (8)

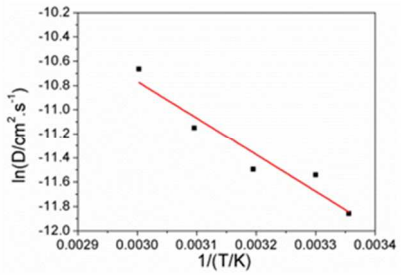

Fig. 9. The shift of lnD(T) with 1/T for the reduction reaction of VO_2^+ on the graphite electrode.

All the above results indicate that the increase of temperature can promote the VO_2^+/VO^{2+} redox reaction and quicken the mobility of VO^{2+} and VO_2^+ ions in the sulfuric acid solutions, suggesting the higher temperature encourages the better performance of VRFB. However, in consideration of the possible precipitation of V (V) ions at a higher temperature,[32] the optimal operation temperature in the VRFB is around 30-40 °C.

4. Conclusions

The elevated temperature facilitates the VO_2^+/VO^{2+} redox reaction, with the rate constants in the order of magnitude of 10^{-3} cm s^{-1}. Temperature has no significant effect on the reversibility of the VO_2^+/VO^{2+} redox couple, while increasing temperature quickens the mobility of vanadium ions in sulfuric acid solutions. Based on the chronopotentiometric results, the diffusion coefficient of VO^{2+} ions increases from 7.39×10^{-6} at 30°C to 8.61 $\times10^{-6}$ cm^2 s^{-1} at 60°C, and that of VO_2^+ ions from 7.07×10^{-6} at 25°C to 23.4 $\times10^{-6}$ cm^2 s^{-1} at 60°C. The corresponding diffusion activation energy for VO^{2+} and VO_2^+ ions in sulfuric acid solutions is 4.24 and 25.2 kJ mol^{-1}, respectively. Therefore, the diffusion equation for VO^{2+} and VO_2^+ ions in sulfuric acid solutions can be expressed by $D_{VO}^{2+} = 4\times10^{-5}$ exp (- 4240/*RT*) and D_{VO2}^{+}=0.18861exp (-25200/*RT*) ($cm^2.s^{-1}$), respectively. The performance of VRFB can be promoted with the increase of temperature, and thus the optimal operation temperature of the VRFB is suggested to be around 30-40°C. These fundamental results will be helpful for understanding the kinetic processes and guiding the engineering application of VRFB.

Acknowledgements

The project was supported by National Basic Research Program of China (2010CB227203) and Natural Science Foundation of Liaoning Province (O4F0A111A7). The authors also would like to thank Dr. Huijun Liu for useful discussions in this paper.

Notes and references

Institute of Metal Research, Chinese Academy of Sciences, 62 Wencui Road, Shenyang, China Fax: 86-024-24508517; Tel: 86-024-24508517; E-mail: xzfan@imr.ac.cn

References

1 H. S. Chen, T. N. Cong, W. Yang, C. Q. Tan, Y.L. Li, Y.L. Ding, *Prog. Nat. Sci.*, 2009, 19, 291.
2 B. Turker, S. A. Klein, L. Komsiyska, J. J. Trujillo, L. von Bremen, M. Kühn, M. Busse, *Energy Convers. Manage*, 2013, 76, 1150.
3 A. Poullikkas, Renew. Sust. *Energy Rev.*, 2013, 27, 778.
4 W. Wang, Q. Luo, B. Li, X. Wei, L. Li, Z. Yang, *Adv. Funct. Mater.*, 2012, 23, 970.
5 M. H. Chakrabarti, N. P. Brandon, S. A. Hajimolana, F. Tariq, V. Yufit, M. A. Hashim, M. A. Hussain, C.T.J. Low, P.V. Aravind, *J. Power Source*s, 2014, 253, 150.
6 Y. Shao, X. Wang, M. Engelhard, C. Wang, S. Dai, J. Liu, Z. Yang, Y. Lin, *J. Power Sources*, 2010, 195, 4375.
7 B. Sun, M. Skyllas-Kazacos, *Electrochim. Acta*, 1992, 37, 2459.
8 B. Sun, M. Skyllas-Kazacos, *Electrochim. Acta*, 1992, 37, 1253.
9 J. Friedl, C. M. Bauer, A. Rinaldi, U. Stimming, *Carbon*, 2013, 63, 228.
10 A. Di Blasi, O. Di Blasi, N. Briguglio, A. S. Aricò, D. Sebastián, M. J. Lázaro, G. Monforte, V. Antonucci, *J. Power Sources*, 2013, 227, 15.
11 W. Y. Li, J. G. Liu, C. W. Yan, *Carbon*, 2013, 55, 313.
12 W. Zhang, J. Xi, Z. Li, H. Zhou, L. Liu, Z. Wu, X. Qiu, *Electrochim. Acta*, 2013, 89, 429.
13 E. Sum, M. Rychcik, M. Skyllas- kazacos, *J. Power Sources*, 1985, 16, 85.
14 H. Kaneko, K. Nozaki, Y. Wada, T. Aoki, A. Negishi, M. Kamimoto, *Electrochim. Acta*, 1991, 36, 1191.
15 S. Iwasa, Y. Wei, B. Fang, T. Arai, M. Kumagai, *Battery Bimonthly*, 2003, 33, 339.
16 Y. Wen, H. Zhang, P. Qian, P. Zhao, H. Zhou, B. Yi, *Acta Phys-Chim Sin.*, 2006, 22, 403.
17 Z. He, J. Liu, H. Han, Y. Chen, Z. Zhou, S. Zheng, W. Lu, S. Liu, Z. He, *Electrochim. Acta*, 2013,106,556.
18 M. Vijayakumar, W. Wang, Z. Nie, V. Sprenkle, J. Hu, *J. Power Sources*, 2013, 241, 173.
19 H.J. Liu, Q. Xu, C.W. Yan, Y.Z. Cao, Y.L. Qiao, *Int. J. Electrochem. Sci.*, 2011, 6, 3483.
20 T. Yamamura, N. Watanabe, T. Yano, Y. Shiokawa, *J. Electrochem. Soc.*, 2005, 152, A830-A836.
21 G. Oriji, Y. Katayama, T. Miura, *J. Power Sources*, 2005, 139, 321.
22 S. Zhong, M. Skyllas-Kazacos, *J. Power Sources*, 1992, 39, 1.
23 G. Oriji, Y. Katayama, T. Miura, Electrochim. Acta, 2004,49, 3091.
24 D. Aaron, C. N. Sun, M. Bright, A.B. Papandrew, M.M. Mench, T.A. Zawodzinski, *ECS Electrochem. Lett.*, 2013, 2, A29.
25 M. Gattrell, J. Park, B. MacDougall, J. Apte, S. McCarthy, C.W. Wu, *J. Electrochem. Soc.*, 2004, 151, A123.
26 M. Gattrell, J. Qian, C. Stewart, P. Graham, B. MacDougall, *Electrochim. Acta*, 2005,51, 395.
27 W. Wang, X. Fan, J. Liu, C. Yan, C. Zeng, Abstract E1-64, 2014 Electrochemical Conference on Energy & the Environment (ECEE), The Electrochemical Society, 2014.
28 W. Wang, X. Fan, J. Liu, C. Yan, C. Zeng, *J. Power Sources*, 2014, 261, 212.
29 A. J. Bard, L. R.Faulkner, *Electrochemical Methods-Fundamentals and Applications*, second ed., Wiley-Interscience, New York, 2001.
30 H. L. Hu, N. Li, *Electrochemical Measurements*, National Defense Industry Press, Beijing, 2011.
31 Q. X. Zha, *An Introduction to Electrode Process Kinetics*, third ed., Science Press, Beijing, 2002.
32 M. Vijayakumar, L. Li, G. Graff, J. Liu, H. Zhang, Z. Yang, J. Z. Hu, *J. Power Sources*, 2011, 196, 3669.

